Seismic Evaluation of Full-Moment Connection CISS Piles/Foundation Systems

Pedro F. Silva[1]

Abstract

Analytical models were developed to evaluate the seismic performance of laterally loaded pile groups. During this evaluation a pile group was modeled and evaluated under different sets of analytical parameters. The following conditions were investigated in the seismic analysis of pile groups using cast-in-place-steel-shell (CISS) piles: (a) soil-structure horizontal stiffness interaction, and (b) soil-structure vertical stiffness interaction. This study shows that variations in the horizontal and vertical soil stiffness affect the pile cap lateral deflection and rotation, respectively, which increase the displacement ductility capacity of bridge column/foundation systems. Results from this study are presented in this paper.

Introduction

One of the main advantages in using steel shells, especially in seismic regions, is the satisfactory performance of steel casings to enhance the ductility capacity of reinforced concrete sections through confinement of the concrete core (Chai et al. 1991; Priestley et al. 1995a). While the seismic response of steel jacketed bridge columns is well understood, uncertainties in the seismic evaluation of cast-in-place-steel-shells (CISS) pile foundation systems still exists due to the complexity of determining the capacity of individual CISS piles in the connection to the pile cap. Analytical models for full moment connection CISS piles were used to evaluate the seismic performance of laterally loaded pile groups (Silva and Seible 2001a). In order to illustrate the applicability of the study presented in this paper, a 4x4 pile group was selected and evaluated under lateral loads using these analytical models. Variables investigated were: (a) soil-structure horizontal stiffness interaction, and (b) soil-structure vertical stiffness interaction. Analytical results indicate that topics discussed in item (a) above, tend to affect significantly the lateral deflection of the pile group, and topics discussed in item (b) tend to affect mostly the rotation of the pile cap. This paper presents a discussion of these analytical results that deal with the seismic performance of CISS pile foundation systems and their influence on the seismic response of bridge systems.

Full-Moment Connection CISS Piles

Full-moment connection CISS piles are typically constructed using steel shells that are embedded into the pile cap, and the core is filled with concrete that is reinforced with straight anchor bars into the pile cap. The prototype CISS pile shown in Figure 1

---

[1] Assistant Prof., Dept. of Civil Arch. and Env. Eng., University of Missouri Rolla

depicts a full-moment connection. The pile shown is the standard Caltrans Class 200 pile (Caltrans 1990). The steel shell is 19mm thick with an inside diameter of 610mm. The core is symmetrically reinforced with ten D35 (US #11) straight anchor bars with a development length of 1346mm. Other design details are depicted in Figure 1b. For this pile type the maximum allowable design axial tension and compression loads are, respectively, −1780kN and +3560kN (Caltrans 1990), where negative values correspond to tensile axial loads and positive values to compressive axial loads.

Analytical Models

Analytical models were developed based on the forces and the stress profiles shown in Figure 2. These profiles were used to fully characterize the load deformation response of the prototype CISS piles along the subgrade and anchorage regions. These analytical models were calibrated using experimental results of the prototype CISS pile depicted in Figure 1 (Silva et al. 1997). A brief description of these analytical models is presented next; however, these models are presented in greater detail elsewhere (Silva and Seible 2001a).

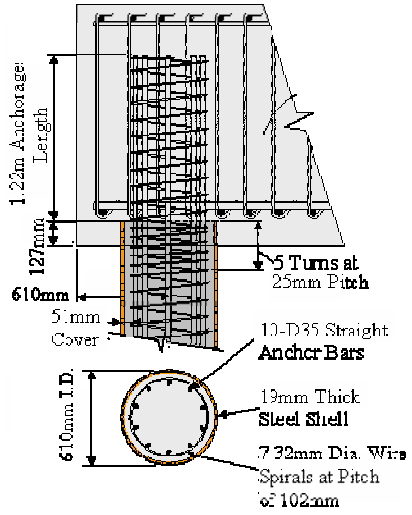

Figure 1 Prototype CISS Piles

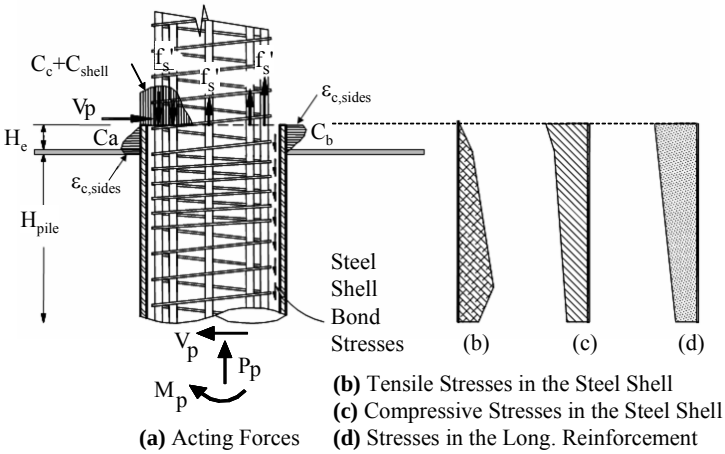

Figure 2 Anchorage Region Force Equilibrium Relations

Section Analysis OUTSIDE the Anchorage Region: Outside the anchorage region and along the subgrade region the lateral load capacity was obtained in terms of the following equilibrium relations (Silva and Seible 2001a)

$$\Sigma C_c + \Sigma C_{s'} + \Sigma C_{shell} = \Sigma T_s + \alpha_{bond} \Sigma T_{shell} + P_p \qquad \text{Eq. (1)}$$

In Eq. (1) the concrete infill forces, ΣC_c, were evaluated considering the confining action of the steel shell (Chai et al. 1991). Within the region near the pile cap, the longitudinal reinforcement tension, ΣT_s, and compression forces, $\Sigma C'_s$, were also

considered in evaluating the moment-curvature capacity of the prototype pile. In regions below the termination of the anchorage reinforcement only the steel shell and the confined concrete forces were considered in evaluating the moment-curvature capacity of CISS piles. Referring to Figure 2 it can be seen that the steel shell is not anchored into the pile cap. As such, the tensile forces present in the steel shell, $\alpha_{bond}\,\Sigma T_{shell}$, were assumed to vary linearly along the development length of the steel shells. The bond factor variable, α_{bond}, varied from *one* at the end of the development length to *zero* at the end of the steel shell inside the pile cap. However, the steel shell was always assumed effective in carrying compression forces because it is directly in contact with the concrete.

Section Analysis WITHIN the Anchorage Region: In the anchorage region the force equilibrium equations used to compute the capacity of the prototype CISS pile were established by Eq. (1). However, the steel shell is not fully anchored into the anchorage region, and as a result the steel shell tension forces are neglected. The moment capacity in the anchorage region was estimated by

$$M_p = \sum T_s D_j - 0.2\,NA \sum C + \Delta M_p + P_p \frac{D_j}{2} - V_p H_e \qquad \text{Eq. (2)}$$

Variables M_p, V_p, and P_p are, respectively, the pile moment, shear and axial forces below the pile cap interface, ΣC is the summation of all the compression forces depicted on the left hand side of Eq. (1), where the centroid of these compression forces was assumed to be located at 0.2*NA* from the section edge, and *NA* is the section neutral axis. Furthermore, in Eq. (2), increase in the flexural capacity due to contact of the steel shell with pile cap cover concrete, ΔM_p, was estimated by

$$\Delta M_p = C_a \frac{H_e}{3} \qquad \text{Eq. (3)}$$

Compression forces C_a developed as a result of the rotation of the steel shell and contact against the pile cap cover concrete.

Moment-Curvature Relations

Moment-curvature relations in the anchorage region were established for the full moment connection prototype pile using the analytical models presented in the previous section. A brief discussion of the performance limit states that were established to characterize the seismic performance of the prototype CISS pile are discussed next. A complete description of these limit states is also presented elsewhere (Hose et al. 2000).

Pile Elastic Limit State: This limit state was defined based on the theoretical first yield of the anchorage reinforcement corresponding to a steel strain of $\varepsilon_s=\varepsilon_y$.

Pile Cap Damage Limit State: A limit state according to the damage observed in the pile cap anchorage region was identified, which corresponds to a pile cap concrete strain of 0.004m/m, and is identified as $\varepsilon_{c.sides}$ in Figure 2. Typical damage observed at this limit state is depicted in Figure 3 (Silva and Seible 2001a), which shows that damage in the pile cap surrounding the steel shell is likely to occur because of the prying action of the steel shell against the pile cap cover concrete.

Figure 3 Pile Cap Damage in the Anchorage Region

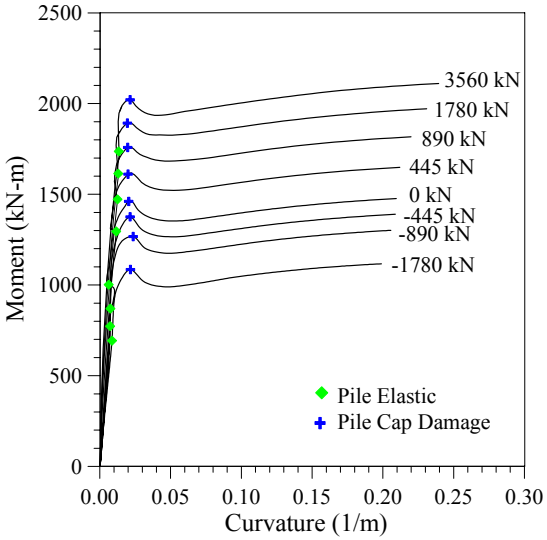

Figure 4 Anchorage Region Moment-Curvature Analyses

A moment-curvature capacity evaluation of the prototype CISS pile in the anchorage region was performed according to the analytical models previously described. These relations were than used in the next section to evaluate the response of pile groups under lateral loads. Analytical results depicted in Figure 4 were computed based on Eq. (1) to Eq. (3), in which the concrete cover and core regions were both assumed fully confined by the steel shell. The numerical values shown near each curve in Figure 4 indicate the different axial load levels used in the analyses (Silva and Seible 2001b). Concrete and steel material properties used in the analysis are presented in Table 1.

Table 1 Material Properties

	Longitudinal Reinforcement		Transverse Reinforcement		Concrete Strength
	f_y MPa	f_u MPa	f_y MPa	Spacing mm	f'_c MPa
Column	400	600	400	100	35
Pile	400	600	400- Spirals 270 – Shell	100	25

Another observation of the moment curvature analyses indicates that the moment capacity of the pile increases significantly beyond the *Pile Elastic Limit State* and up to

the *Pile Cap Damage Limit State* due to the prying action of the steel shell, as obtained in terms of Eq. (3). The *Pile Cap Damage Limit State* is followed by a decrease in the moment capacity, as a result of damage in the vicinity of the pile, as depicted in Figure 3. This condition matches with experimental results (Silva and Seible 2001a).

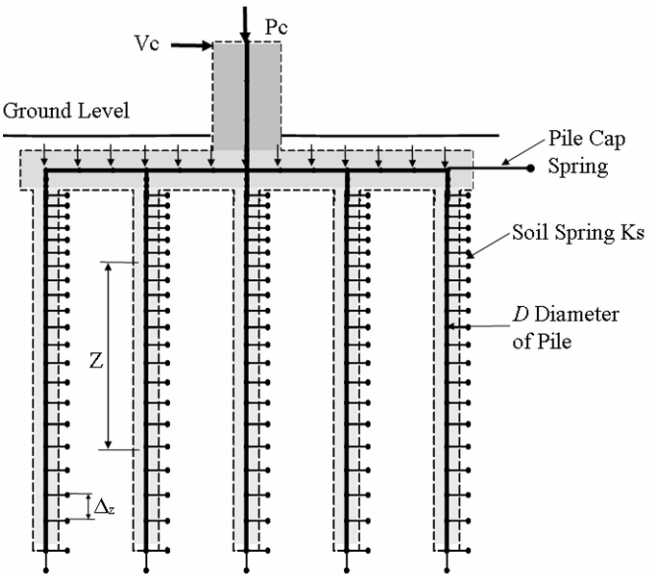

Figure 5 Pile Group Finite Element Model

Pile Group Analytical Modeling

In this study, the pile group was investigated in terms of: (1) horizontal stiffness of the soil at the level of the pile cap and surrounding the piles, and (2) soil to pile vertical stiffness interaction. The finite element model used in the pile group analysis is presented in Figure 5. In the finite element model the piles were modeled according to the properties for the standard Caltrans Class 200 pile with a steel shell embedment length of 127mm. The piles were arranged in a 4x4 pile group with centerline spacing of 1.55m and an edge distance to the pile cap of 0.61m.

The column height was modeled as 6.0m. Variations in the column height will affect the response of the pile group. However, to reduce the paper content this condition was not discussed in further detail in this paper. The column was modeled according to the characteristics shown in Figure 6. In addition, the pile cap was modeled as linear elastic with the stiffness computed based on a section with dimensions of 5.87m x 5.87m x 0.61m. Concrete and steel material properties used in the analysis of the pile group are presented in Table 1.

The soil structure interaction analysis was performed using the pushover analysis technique. The analytical component of the study was then conducted by interfacing a moment curvature analysis program with a finite element program. The finite element package that was used in conjunction with the moment-curvature program was the structure analysis program CALSD developed at UCSD (Seible *et al.* 1991). The interface between the moment curvature and the finite element program was accomplished via batch mode at incremental steps of analysis.

Single Pile Modeling

The analytical subgrade reaction model, typically known as the Winkler model, was used for the analysis of piles under lateral loading (Fleming *et al.* 1985). Soil-

structure interaction analysis was performed using beam elements for modeling of the piles, and the soil surrounding the piles was modeled with truss elements according to the discrete finite element model illustrated in Figure 7.

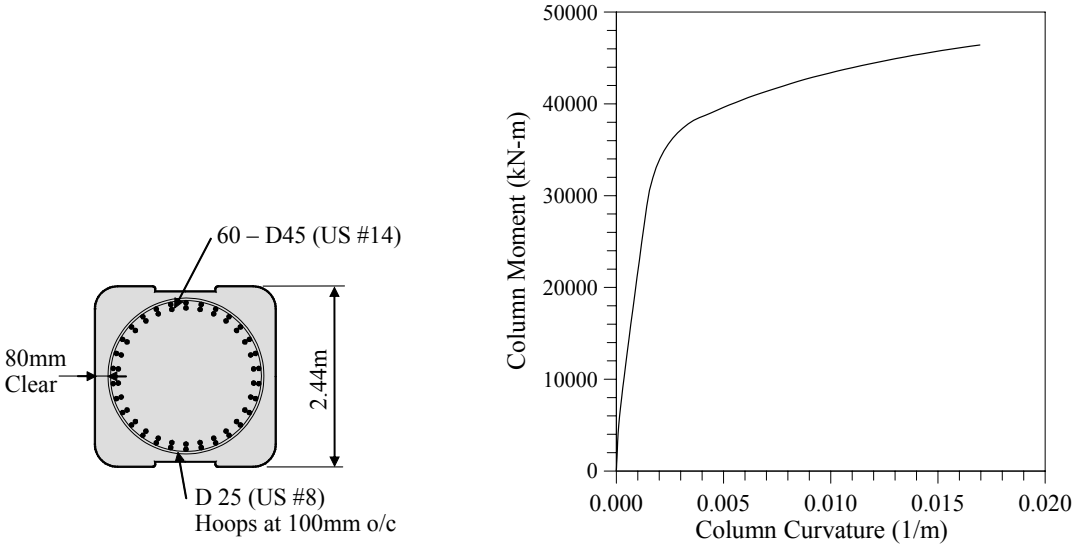

(a) Column Cross-Section (b) Column Moment-Curvature Relations

Figure 6 Column Cross Section

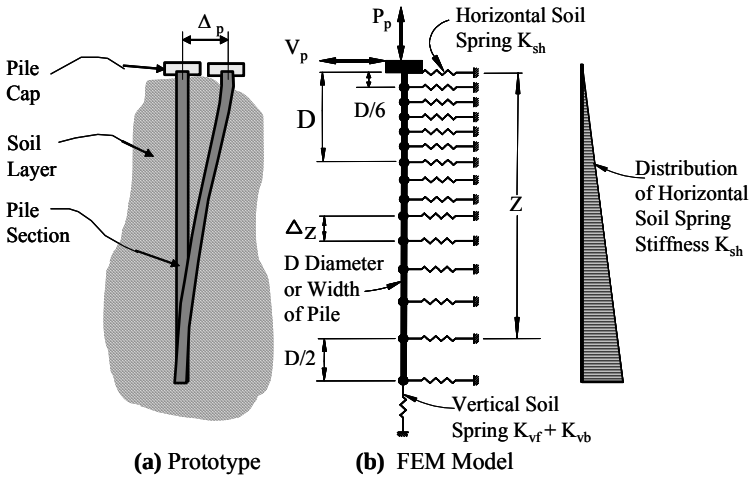

Figure 7 Finite Element Model of Single Piles

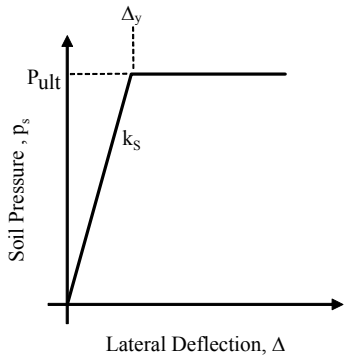

Figure 8 Bilinear Soil Model

It can be shown that the accuracy in the finite element model concerning the lateral response of piles is directly dependent on the pile discretization. In this study, six beam elements with a length of D/6 were used at the pile head, and using a quadratic regression, the element sizes were increased to D/2 at the pile tip elevation, as shown in Figure 7. The anchorage zone was modeled by a single element positioned at the upper most location connection to the pile cap. The bending stiffness of this single element was obtained using the moment curvature relations previously described. In this model, at each load increment the pile beam elements bending stiffness properties were updated

based on the moment curvature analyses, and the soil was modeled as an array of uncoupled spring elements.

Soil Modeling

Horizontal Soil Model Surrounding Piles: Effects of the soil surrounding the piles in the horizontal direction were modeled in terms of elements with axial stiffness only. These elements were placed only on one side of the pile with equal axial stiffness in compression and tension. A bilinear relation between the horizontal soil pressure and lateral displacement, as shown in Figure 8, was used to idealize the soil strength. The analyses described in this section were performed using the soil types described in Table 2. The bilinear horizontal soil model expressed in terms of the soil pressure was given by (Pender 1978; Poulos 1971)

$$p_s = k_S \ \Delta_z; \qquad p_s \le p_{ult} \qquad \text{Eq. (4)}$$

The soil spring stiffness at any depth was obtained according to the relation

$$K_{sh} = k_S \ \Delta_z \ Z \qquad \text{Eq. (5)}$$

Where K_s is the equivalent spring stiffness, k_S is the coefficient of subgrade reaction given in kN/m^3, and Δ_Z is the spacing between the springs at a depth Z. Assuming the coefficient of subgrade reaction was normalized in terms of a nominal pile diameter of 1.80m (Priestley *et al.* 1995b), then k_S may be expressed in terms of the nominal pile diameter D^* and the pile section diameter D. Thus, the soil normalized spring stiffness was given by

$$K_{sh} = k_S \ \Delta_z \ Z\left(\frac{D}{D^*}\right) \qquad \text{Eq. (6)}$$

In Eq. (4) the limiting soil pressure, p_{ult}, was obtained according to the relation (Fleming 1985)

$$p_{ult} = 5 \ K_p \ \sigma'_v \qquad \text{Eq. (7)}$$

$$K_p = \frac{1+\sin\varphi_s}{1-\sin\varphi_s} \qquad \text{Eq. (8)}$$

Where K_p, is the passive earth pressure coefficient, φ_s is the soil friction angle, which for sands is usually taken as 35^o. Based on this soil friction angle, K_p then has a value of 3.70. In Eq. (7) σ'_v is the vertical effective stress at a depth Z expressed in terms of the soil unit weight, γ, by the relation

$$\sigma'_v = \gamma Z \qquad \text{Eq. (9)}$$

Change of the soil properties during cyclic response may lead to permanent deformations in the soil layer, and the soil ultimate strength and stiffness decay with each cycle. An analytical approach developed by Matlock used a gap element (Matlock and Reese 1969). However, this gapping phenomenon was also not covered in this work.

Table 2 Soil Types

Soil Type	Coefficient of Subgrade Reaction, k_S kN/m^3
Soft	3000
Stiff	30000

Horizontal Soil Model Surrounding Pile Cap: The seismic response of the pile group was also characterized in terms of the passive pressure that develops in front of the pile cap. This was conducted by positioning a spring in front of the pile cap as illustrated in Figure 5. The pile cap spring stiffness was computed according to the expression

$$K_{cap} = k_S \frac{H_{cap}^2}{2}\left(\frac{W_{cap}}{D^*}\right) \qquad \text{Eq. (10)}$$

Where H_{cap} and W_{cap} are the height and width of the pile cap, respectively.

Vertical End Bearing Stiffness: The soil structure interaction in the vertical direction of the piles was modeled using vertical elements with axial stiffness. Modeling of the soil-structure interaction in the axial direction is described next. The vertical end bearing stiffness, K_{vb}, (only for piles in compression) was given by

$$K_{vb} = k_S \frac{D}{2} L\left(\frac{D}{D^*}\right) \qquad \text{Eq. (11)}$$

This expression is similar to Eq. (6) but the distance between the springs is equal to half the pile diameter. This indicates that the vertical end bearing resistance was modeled equally to the horizontal spring stiffness, which is located at the bottom of the piles.

Vertical Skin Friction Resistance Stiffness: The vertical skin friction resistance stiffness, Kvfi, was given by (Pender 1978; Poulos 1971)

$$K_{vfi} = 1.8\, E_{s-tip}\, \eta\, \lambda^{(0.5-\lambda/\eta)}\alpha \qquad \text{Eq. (12)}$$

Where η is the pile ratio, and λ is the pile-soil stiffness ratio given by

$$\eta = \frac{L}{D} \qquad \text{Eq. (13)}$$

$$\lambda = \frac{E_p}{E_{s-tip}} \qquad \text{Eq. (14)}$$

Where E_{s_tip} is the soil young modulus at the pile tip. In Eq. (12) α is an expression that was used in order to distribute the effects of the soil vertical stiffness along the length of the piles. As described in this section these elements were positioned along the piles according to these different conditions: (1) a single vertical spring was positioned at the bottom of the piles (see Figure 9a), and (2) springs were distributed vertically along the length of the piles (see Figure 9b). These conditions are described next.

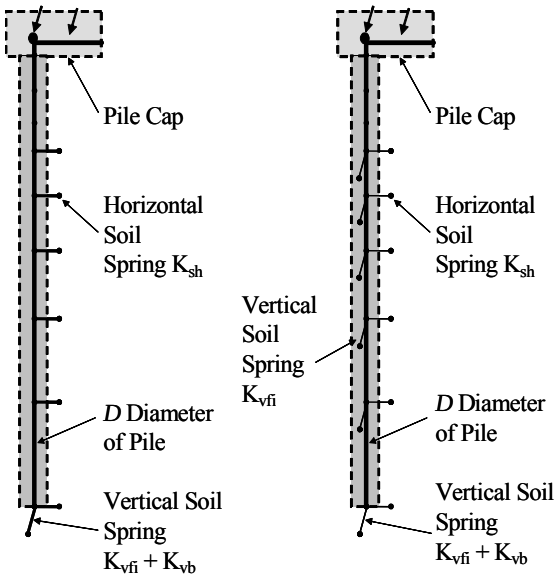

Figure 9 Models for Vertical Soil Springs

Single Vertical Spring at Bottom of Piles: For the condition where a single vertical spring was positioned at bottom of the piles α=1.00. In this case the vertical soil structure interaction (i.e. skin friction and end bearing) formulation was defined as depicted in Figure 9a.

Distributed Vertical Springs Along Length of Piles: For distributed vertical springs positioned along the full length the total skin friction resistance given by the piles α is given by

$$\alpha = \frac{Z\ \Delta_z}{L^2} \qquad \text{Eq. (15)}$$

In Eq. (15) α is significantly smaller than 1 and summation of all α's along the length of the pile is nearly 1.00, which indicates that the total stiffness given by these two approaches are similar and can be compared directly. In addition, the vertical stiffness increases along the length of the piles in terms of the relation *Z/L*, which is to take into account the change in the soil Youngs's modulus along the length of the piles.

Pile Group Analysis Results

Analytical results to characterize the response of the pile group based on the conditions previously defined are presented next. It can be shown that the performance of a pile group may be evaluated in terms of the pile cap rotation and lateral deflection.

Pile Cap Rotation: Figure 10 presents the cap beam rotations for different cap beam soil spring stiffness and for stiff and soft soils. Soil properties for these two soil types are presented in Table 2. The following are some observations derived from Figure 10.

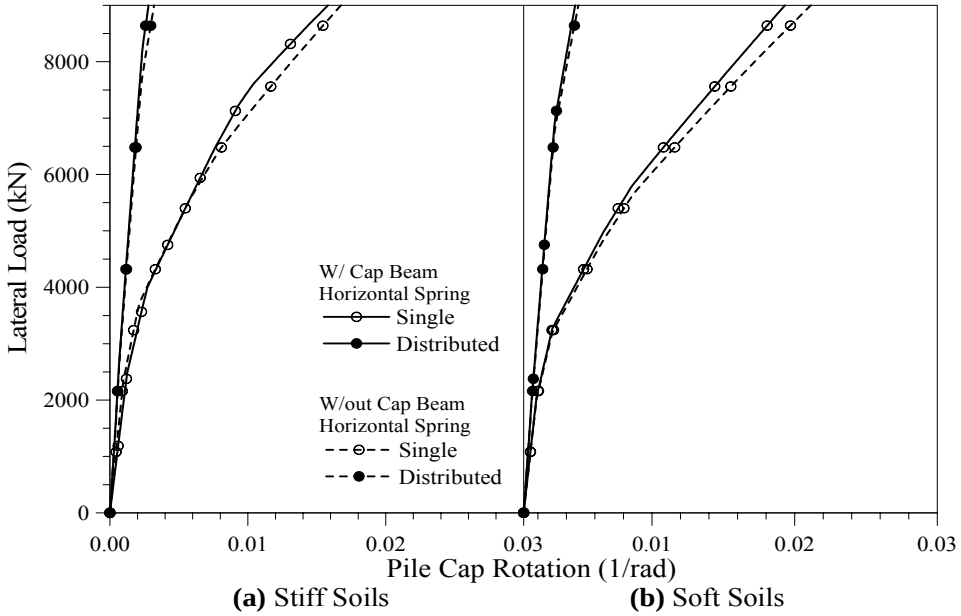

Figure 10 Pile Group Analysis – Pile Cap Rotation

1. The horizontal spring positioned at the front of the pile cap, K_{cap}, have minimum effect on the pile cap rotation. In this figure it is clear that modeling with and without this spring in front of the pile cap (represented with solid and dashed curves) leads to nearly the same pile cap rotations.

2. The horizontal soil stiffness placed along the length of the piles has a minimum affect on the pile cap rotation. This was deduced by comparing results presented in Figure 10a and Figure 10b. These figures show that for stiff and soft soils the pile cap rotation are nearly identical for the same conditions modeling the soil in the horizontal direction.

3. Modeling of the vertical springs, which describe the interaction of the pile-soil skin friction and pile tip bearing resistance, has a significant impact on the pile cap rotation. Referring to Figure 10 it is clear that modeling with a single spring (represented

by the open circles) leads to significantly higher pile cap rotations than modeling with distributed springs (represented by the closed circles).

Pile Cap Lateral Deflection: As before, Figure 11 presents the cap beam lateral deflection for different cap beam soil spring stiffness and for stiff and soft soils. The following are some observations derived from Figure 11.

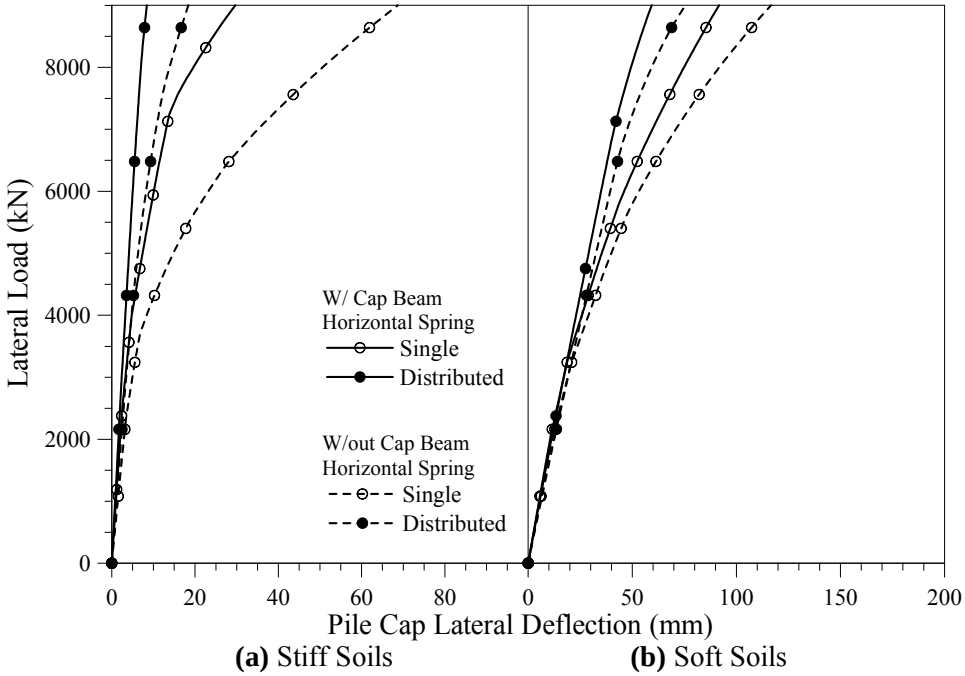

Figure 11 Pile Group Analysis – Pile Cap Lateral Deflection

1. The horizontal springs positioned at the front of the pile cap affects significantly the pile cap lateral deflection. From this figure it is clear that the pile cap lateral deflection was significantly larger when the pile cap horizontal spring was not considered in the analysis; however, this difference was more accentuated for soft soil conditions.

2. The horizontal soil stiffness placed along the length of the piles also has a significant impact on the pile cap lateral deflection. As before, this observation was deduced by comparing results presented in Figure 11a and Figure 11b for stiff and soft soils, respectively. These figures show that the pile cap lateral deflection was larger for soft soil conditions.

3. Modeling of the vertical springs only imposes a small difference on the pile cap lateral deflection. Referring to Figure 11 it is clear that modeling with a single spring (represented by the open circles) leads to similar pile cap lateral deflection than modeling with distributed springs (represented by the closed circles).

These observations indicate that generally modeling of the horizontal spring stiffness have a higher influence on the pile cap lateral deflection. On the other hand, the vertical spring stiffness, either at the pile ends or along the length of the piles, have a higher influence on the pile cap rotation.

Conclusions

Analytical studies were presented in this paper that can serve to characterize the seismic performance of full-moment connections CISS pile foundation systems. The following conclusions describe key findings:

1. The embedment of steel shells into the pile cap significantly affects the lateral response of CISS piles in the anchorage region. Corroborated by experimental evidence, due to the embedment of the steel shell into the pile cap it may not be possible to maintain a damage free connection.

2. Parametric studies indicate that the seismic response of pile foundation systems is dependent on the following: (*a*) soil stiffness, (*b*) horizontal passive pressures that are mobilized in front of the pile cap, (*c*) finite element modeling of the soil-structure interaction axial stiffness, and (*d*) column height. However, modeling of the soil-structure interaction horizontal and axial stiffness (items *a* to *c*) were found to influence the most the seismic response of pile foundation systems. Analytical results show that the soil-structure interaction horizontal stiffness affects significantly the pile cap lateral deflection, and in contrast the soil-structure interaction vertical stiffness affects significantly the pile cap rotation.

References

Caltrans (1990) "Bridge Design Specifications - Seismic Design References," Sacramento, California, June 1990.

Chai, H. Y., Priestley, M. J. N., Seible, F. (1991), "Seismic Retrofit of Circular Bridge Columns for Enhanced Flexural Performance," *ACI Journal Journal*, Vol. 88, No.5, Sept. - Oct. 1991, pp. 572-584.

Fleming, W. G. K., Weltman, A. J., Randolph, M. F., Elson, W. K. (1985), *Piling Engineering,* John Wiley & Sons, Inc., New York, 1985.

Hose, Yael D., Silva, P. F., Seible, F. (2000), "Performance Evaluation of Concrete Bridge Components and Systems under Simulated Seismic Loads," *EERI Earthquake Spectra*, Vol. 16, No. 2, May 2000, pp. 413-442.

Matlock, H., Reese, L.C., (1969) "Generalized Solutions For Laterally Loaded Piles," ASCE Journal of the Soil Mechanics and Foundations Division, Vol. 86, No. SM5, October 1969, pp. 63-91.

Pender, M. J., (1978)" *Aseismic Pile Foundation Design Analysis* ," Bulletin of the New Zealand National Society for Earthquake Engineering, Vol. 11, No. 2, June 1978, pp 49 - 160.

Poulos, H. G. (1971), *"Behavior of Laterally Loaded Piles: I - Single Piles, "* Proceedings of the American Society of Civil Engineers, Vol. 97, No. SM5, May 1971, pp. 711-731. - Elastic Continuum Concept

Priestley, M. J. N., Seible, F., Calvi, M., (1995a) *Seismic Design and Retrofit of Bridges,* John Wiley & Sons, Inc., New York, September 1995, 672 page.

Priestley, M. J. N., Budek, A., Benzoni, G. (1995b), An Analytical Study of the Inelastic Seismic Response of Reinforced Concrete Pile-Columns in Conhesionless Soil, Report SSRP 95/13, Department of Structural Engineering, University of California San Diego, La Jolla, CA, March 1995.

Seible, F., Kurkchubasche, A., Mazzoni, S. (1991), "CALSD Instructional Computer Programs for Structural Engineering," University of California San Diego, California, January 1991.

Silva, P. F., Seible, F., Priestley, M. J. N., (1997) Response of Standard Caltrans Pile-to-Pile Cap Connections Under Simulated Seismic Loads, Report SSRP 97/09, Department of Structural Engineering, University of California San Diego, La Jolla, CA, November 1997.

Silva, P. F., Seible, F. (2001a), "Seismic Performance Evaluation of CISS Piles," *ACI Structural Journal*, Vol. 98, No. 1, January 2001, pp. 36-49.

Silva, P. F., Seible, F. (2001b), "Experimental Procedure for Testing of Piles Under Varying Axial and Lateral Loads," *SME Experimental Techniques Journal*, Vol. 25, No. 1, February 2001, pp. 25-30.